Supramolecular Polymers

DOI: 10.1002/anie.201108466

Organogold(III) Supramolecular Polymers for Anticancer Treatment**

Jing-Jing Zhang, Wei Lu, Raymond Wai-Yin Sun, and Chi-Ming Che**

Supramolecular polymers self-assembled from metal complexes have important and diverse applications in catalysis[1] and materials science.[2] The properties and applications of metal-containing supramolecular polymers can be altered by metal ions and/or by ligands with various functionalities. Complexes of Cu^{I}, Cu^{II}, Pd^{II}, Co^{II}, Pt^{II}, and Au^{I} are known to self-assemble into functional polymeric nanostructures that display intriguing physical and/or chemical properties.[3] In contrast, medicinal applications of metal-based supramolecular polymers have been sparsely reported. A notable example is a biocompatible supramolecular polymer formed by coordination of Gd^{III} ions to a tetraazamacrocyclic moiety attached to peptide scaffolds, which has useful applications in magnetic resonance imaging.[4]

Gold complexes with promising in vitro and in vivo anticancer activities have been receiving much attention as metal-based anticancer medicines.[5,6] Some Au^{III} complexes of N-confused porphyrins and corroles were suggested to display phototoxicity.[7] We recently showed that Au^{III} porphyrins[6] and $[Au^{III}_{n}(C\text{^}N\text{^}C)_{n}(L)]^{n+}$ complexes (HC^N^CH = 2,6-diphenylpyridine; $n = 1$ or 2; L = phosphine[8b] or *N*-heterocyclic carbene[8a]) display potent in vitro and in vivo anticancer activity. In clinical applications, the high toxicity of gold complexes is a major issue yet to be resolved.[9] We conceive that sustained release of anticancer-active Au^{III} complex from drug-carrying capsules could be a useful approach to decrease the initial high concentration of cytotoxic Au^{III} complex and thus reduce its toxicity towards normal cells.[10]

We were attracted to a recent report on supramolecular hydrogels formed from *N*-acetyl-L-cysteine and $HAu^{III}Cl_4$.[11] Unfortunately, the low pH at which these hydrogels were formed (pH < 4) limits their applications in biological systems. Herein we report a dual-functionalized supramolecular polymer self-assembled from a cyclometalated Au^{III} complex containing a hydrogen-bonding motif and its potential application in anticancer treatment. The present study features the first example of the medicinal application of a self-assembled organogold(III) supramolecular polymer. The sustained cytotoxicity of $[Au^{III}(C\text{^}N\text{^}C)(4\text{-dpt})](CF_3SO_3)$ (**1**; 4-dpt = 2,4-diamino-6-(4-pyridyl)-1,3,5-triazine; Scheme 1) and carrier properties of the supramolecular

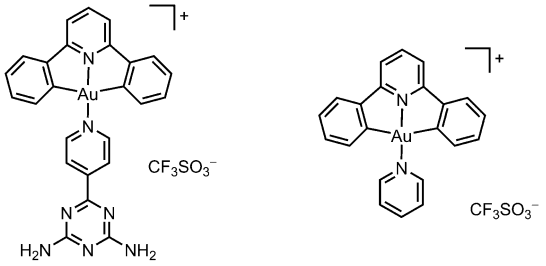

Scheme 1. Chemical structures of Au^{III} complexes **1** and **2**.

nanofibers were examined. The anti-angiogenic ligand 4-dpt[12a] may result in the formation of intermolecular hydrogen-bonding and π–π interactions, given that these types of noncovalent interactions were evidenced previously in a self-assembled supramolecular Cu^{II} complex containing the 4-dpt ligand.[12b]

Complex **1** was prepared by treatment of $[Au^{III}(C\text{^}N\text{^}C)Cl]$ with 4-dpt in the presence of $Ag^{I}CF_3SO_3$ in CH_3CN at 308 K. Detailed characterization is given in the Supporting Information (Figures S1–S3). $[Au^{III}(C\text{^}N\text{^}C)(pyridine)](CF_3SO_3)$ (**2**) was also prepared for a comparative study.

Complex **1** was found to self-assemble into a supramolecular polymer (**1-SP**) in CH_3CN. At a concentration of 20 mM, **1** can be dissolved in CH_3CN at 323 K, but the solution turns into a viscous liquid after cooling to 298 K (Figure 1). Complex **2** failed to self-assemble to form a viscous solution mixture under identical conditions, that is, the guanamine-like moiety of the 4-dpt ligand is pivotal for the high viscosity of the solution. In EtOH and DMSO, both **1** and **2** failed to self-assemble into supramolecular polymer (Supporting Information Figure S4). The log–log plot of the concentration-dependent specific viscosity of **1-SP** in CH_3CN measured at 294 ± 1 K (Supporting Information Figure S5) shows a significant increase in viscosity at concentrations above 6.3 $g\,L^{-1}$; this is a typical behavior for a solution of supramolecular

[*] J.-J. Zhang, Dr. W. Lu, Dr. R. W.-Y. Sun, Prof. Dr. C.-M. Che
State Key Laboratory of Synthetic Chemistry, Open Laboratory of Chemical Biology of the Institute of Molecular Technology for Drug Discovery and Synthesis, and Department of Chemistry, The University of Hong Kong, Pokfulam Road, Hong Kong (China)
E-mail: cmche@hku.hk
rwysun@hku.hk
Dr. W. Lu
Department of Chemistry
South University of Science and Technology of China
1088 Xueyuan Boulevard, Shenzhen, Guangdong 518055 (China)

[**] This work is supported by The Innovation and Technology Fund (Tier-2 project, ITS/134/09FP) administrated by The Innovation and Technology Commission and The Area of Excellence Scheme (AoE/P-10/01) established under the University Grants Committee of the Hong Kong Special Administrative Region, China. We thank Dr. Xiangguo Guan for performing the molecular modeling. Thanks go to Frankie Yu-Fee Chan and Amy Sui-Ling Wong at HKU for assistance in electron microscopy.

Figure 1. Photographs showing formation of the viscous fluid (supramolecular polymer) of **1** in CH_3CN. a) Suspension of **1** at 298 K. b) Dissolution of **1** on heating at 323 K. c) Formation of viscous fluid (**1-SP**) after cooling the solution in b) to 298 K.

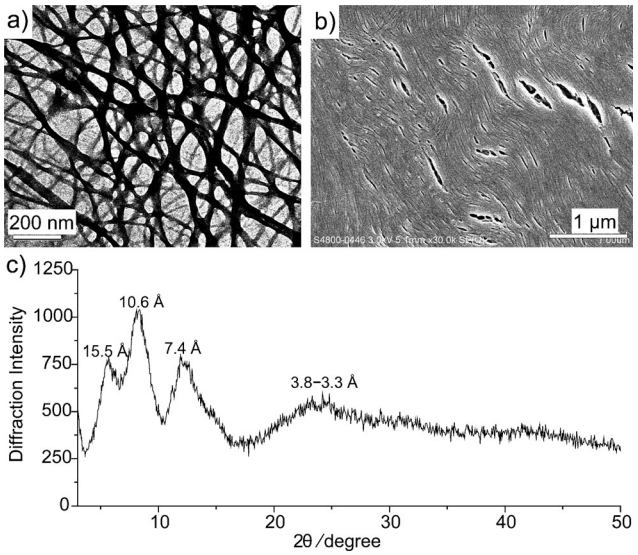

Figure 2. a) TEM image, b) SEM image, and c) powder XRD pattern of **1-SP**.

polymer.[3c] Transmission electron (Figure 2a) and scanning electron micrographs (Figure 2b) of **1-SP** reveal partially aligned nanofibers with diameters and lengths of about 50 nm and tens of micrometers, respectively. Partial entanglement of these nanofibers accounts for the high viscosity at high concentration of **1** (20 mM). The powder XRD pattern of the nanofibers is depicted in Figure 2c. The broad diffraction peaks at 2θ values of 5.69° ($d \approx 15.5$ Å, corresponding to the longest molecular dimension of **1**), 8.31° ($d \approx 10.6$ Å), and 12° ($d \approx 7.4$ Å) could be attributed to partially regular packing of complex **1** in nanofibers. The broad halo centered at $2\theta = 25°$ ($d \approx 3.8$–3.3 Å) can be accounted for by intermolecular π–π stacking interactions between the $[Au^{III}(C^N^C)]$ moieties. A ^1H NMR study on **1** in CD_3CN at different concentrations and temperatures (see Supporting Information Figure S6 for spectra) showed that the signals assigned to the NH_2 protons continuously shifted upfield with decreasing concentration from 20 to 8 mM and increasing temperature from 298 to 322 K, and thus revealed that the amino group of the guanamine-like moiety of the 4-dpt ligand is involved in hydrogen-bonding interactions in the self-assembly of complex **1**. On the basis of these findings, a one-dimensional structure of **1-SP** with alternating hydrogen-bonding and π–π stacking interactions between two cations of **1** is proposed (Supporting Information Figure S7).

A 20 mM solution of **1** in CH_3CN was used to prepare a stock **1-SP** solution with mass content of **1** of 15.26 μg μL^{-1}. The stability of **1-SP** in phosphate-buffered saline (PBS, 10 mM phosphate, 27 mM KCl, 137 mM NaCl, pH 7.4) in the absence or presence of the biological reductant glutathione (GSH, 2 mM) was examined, and the results are summarized in Scheme 2a. In the absence of GSH, absorbance at 274 nm

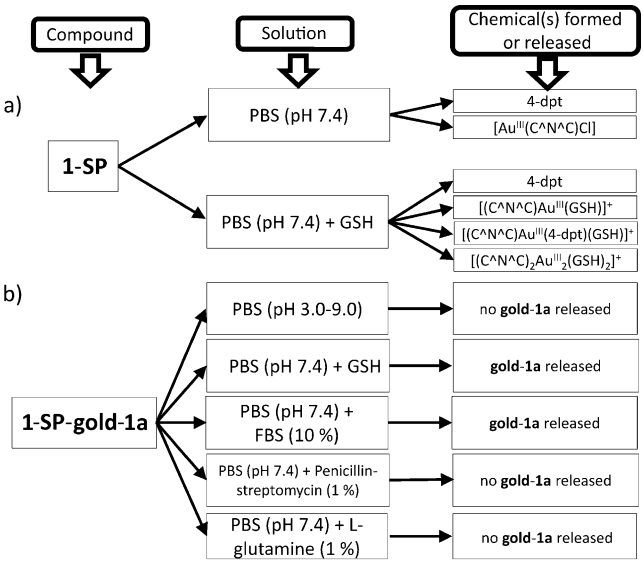

Scheme 2. Controlled-release behavior of a) **1-SP** and b) **1-SP-gold-1a** in different solutions.

gradually increases, as revealed by UV/Vis absorption spectrophotometry (Figure 3a). A white precipitate was found in the solution on prolonged incubation (>24 h). Subsequent ESI-MS and ^1H NMR studies revealed that 4-dpt was released into the solution, and both $[Au^{III}(C^N^C)Cl]$ and 4-dpt contributed to the precipitates (Supporting Infor-

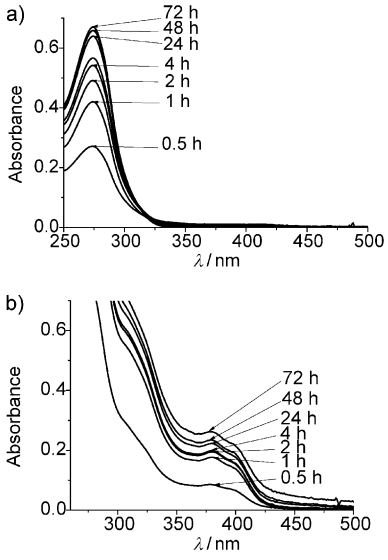

Figure 3. UV/Vis absorption spectral traces (0–72 h) of **1-SP** in PBS (pH 7.4) in a) the absence and b) the presence of GSH (2 mM).

mation Figure S8 and S9). These results suggest that 4-dpt in **1-SP** can be replaced by chloride ion in PBS, with formation of $[Au^{III}(C^N^C)Cl]$ and release of 4-dpt. Unlike **1-SP**, immediate degradation of complexes **1** and **2** to form $[Au^{III}(C^N^C)Cl]$ precipitate occurred in PBS (pH 7.4), and the poor solubility of $[Au^{III}(C^N^C)Cl]$ hampers further biological application of these two complexes. The percentage release of 4-dpt from **1-SP** compared with that from **1** in PBS was studied by UV/Vis spectrophotometry (Supporting Information Figure S10). 4-Dpt was found to be gradually released from 20% to about 75% in the first 10 h, and to about 80% after 24 h. Since 4-dpt was immediately released from **1** in PBS, this release can be used as an indicator for monitoring degradation of the supramolecular assembly. All of these results suggest that **1-SP** would have much higher bioavailability than **1** and **2**. In the presence of GSH, a gradual increase in absorbance between approximately 260 and 380 nm was found (Figure 3b). By ESI-MS analysis, ion cluster peaks were found with m/z values of 189, 733, 920, and 1464, corresponding to $[4\text{-dpt}+H]^+$, $[(C^N^C)Au^{III}(GSH)]^+$, $[(C^N^C)Au^{III}(4\text{-dpt})(GSH)]^+$, and the dimeric species $[[(C^N^C)_2Au^{III}_2(GSH)_2]^+$ (Supporting Information Figure S11).

We further examined the in vitro cytotoxicity of **1-SP** on human cell lines of melanoma (B16) and normal lung fibroblast (CCD-19Lu) in the absence of photoactivation. To avoid direct contact of **1-SP** with the cells, double-chambered Transwell 24-well plates containing a semipermeable membrane at the bottom of the upper chamber were employed in the cytotoxicity assay. Cells were seeded in the lower chambers of the plate. The viscous stock solution of **1-SP** (3.5 μL, corresponding to 20 mM of monomeric complex **1**) diluted with H_2O (10.5 μL) was subsequently placed inside the detachable upper chambers. The semipermeable membrane allowed the released low molecular weight molecules from **1-SP** to diffuse to the cells (Figure 4a). The entire

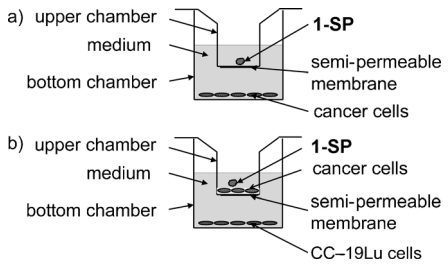

Figure 4. a) Cytotoxicity assay in Transwell 24-well plates for sustained release experiment and b) mimicking intratumoral injection in Transwell 24-well plates.

Transwell 24-well plate was first incubated at 310 K (5% CO_2/95% air). Different sets of the upper chambers, together with the viscous polymer solution, were detached from the lower chambers after 5, 10, 24, 48, or 72 h of incubation. At a total 72 h of incubation, the percentage survival of the cells in each lower chamber was quantified by MTT assay.[13]

As depicted in Figure 5a, percentage survival of the B16 cancer cells (solid line) decreased with increasing co-incubation time of **1-SP**. Since the culture medium was rich in chloride and cancer cells have high concentrations of GSH, we reckon that both the sustainably released free 4-dpt ligand and the $[Au^{III}(C^N^C)]$–GSH adduct(s) account for the sustained cytotoxicity. Contrary to the sustained cytotoxicity of **1-SP**, the cancer cells showed a rapid response to complex **1** or **2** at the same concentration; the percentage death of the cells after 24 h reached more than 80% in both cases (Supporting Information Figure S12). Besides, **1-SP** exhibited cytotoxicity through an apoptotic pathway, and similar findings were made with complexes **1** and **2** (Supporting Information Figure S13). Taken together, these results suggest that **1-SP** could have potential application in sustained-delivery therapy with improved therapeutic efficiency and safety by reducing the frequency of drug administration and the dose of drug required.

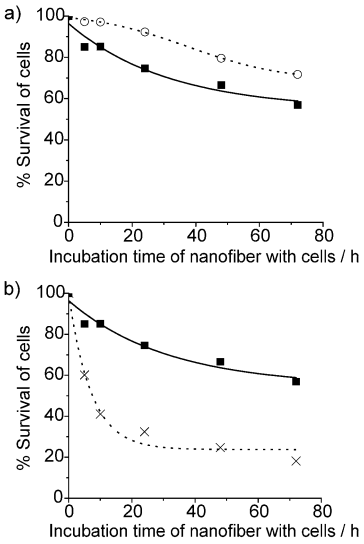

Figure 5. a) Time-dependent cytotoxicity (0–72 h) of **1-SP** toward B16 (solid line) and CCD-19Lu (dotted line) cell lines. b) Time-dependent cytotoxicity (0–72 h) of **1-SP** (solid line) and **1-SP-gold-1a** (dotted line) against B16 cancer cells.

To examine whether **1-SP** has specific selectivity for cancer cells, its cytotoxicity towards CCD-19Lu was examined. Under the same condition, **1-SP** displayed lower cytotoxicity to the fibroblast cells with higher percentage cell viability at different times of incubation (i.e., from 5 to 72 h, Figure 5a). The cancer-cell selectivity of **1-SP** prompted us to further explore its potential therapeutic applications. We hypothesize that **1-SP** could be implanted directly in solid tumor by intratumoral injection to achieve localized drug delivery. In this case, cancerous cells were in close contact with **1-SP**, while normal cells were in a remote area.[14] To mimic this situation in vitro, we employed the Transwell 24-well plates. The **1-SP** was co-incubated with cancerous B16 cells (close contact) in the upper chambers, while normal lung fibroblast cells were placed in the bottom chambers (remote area, Figure 4b). The survival percentages of the cells in the upper and lower chambers were quantified separately. At 100 μM of **1-SP**, less than 15% of the B16 cells remained viable in the upper chambers. In contrast, over 70% of the normal

cells survived in the lower chambers, which were remote from **1-SP**. This result reveals that **1-SP** has potential application in localized drug delivery, which provides higher doses of drug to the target tissue with reduced systemic toxicity.

In addition to its cytotoxicity, **1-SP** can also be used as a carrier for other cytotoxic agents. We chose Au^{III} porphyrin complex $[Au^{III}(TPP)]Cl$ (**gold-1a**; H_2TPP = *meso*-tetraphenylporphyrin), since its anti-cancer properties have been extensively studied.[6] Moreover, this complex shows strong absorption peaks in the UV/Vis region, enabling it to be observed as a reddish species even at low concentration (e.g., 10 μM). We found that the nanofibrillar networks of **1-SP** could act as an encapsulating material by modulating the release of the cytotoxic agent. Encapsulated **gold-1a** (denoted **1-SP-gold-1a**) was prepared by adding aliquots of **gold-1a** to a suspension of **1** in CH_3CN, which was heated at 323 K to form a clear solution. The solution was cooled to 298 K to give the product (Figure 6). SEM revealed that partially aligned and entangled nanofibers were formed (Supporting Information Figure S14).

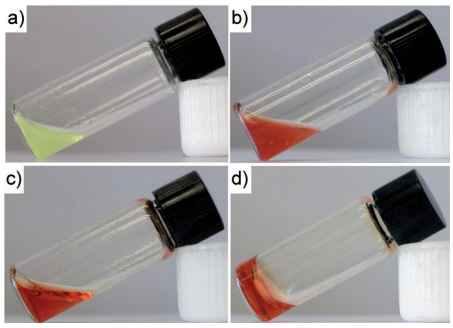

Figure 6. Photographs showing formation of the viscous fluid (supramolecular polymer) of **1** and $[Au^{III}(TPP)]Cl$ (**gold-1a**) in CH_3CN. a) Suspension of **1** at 298 K. b) Addition of **gold-1a** to the suspension. c) Dissolution of **1** and **gold-1a** on heating at 323 K. d) Formation of viscous fluid after cooling the solution in c) to 298 K.

The **gold-1a** was trapped in the **1-SP** in PBS at pH 3.0–9.0 for 72 h, as no apparent release of **gold-1a** to the solution was detected (Supporting Information Figure S15). In contrast, **gold-1a** was gradually released to a PBS solution at pH 7.4 containing GSH (2 mM). As depicted in Figure S16 of the Supporting Information, the UV/Vis absorption spectrum of the GSH solution containing **1-SP-gold-1a** showed gradual increase in absorbance at 380, 420, and 530 nm. The increase in absorbance at 380 nm, as discussed above, is attributed to formation of $[Au^{III}(C\text{^}N\text{^}C)]$–GSH adduct(s). We reckon that the increase in absorbance at 420 and 530 nm is attributed to sustained release of **gold-1a** to the solution, since free **gold-1a** was detected by ESI-MS in the extracted organic layer of the solution (Supporting Information Figure S17). Moreover, the UV/Vis spectral change is also in agreement with the reported spectrum of **gold-1a**.[6] All results are depicted in Scheme 2b. Besides GSH, fetal bovine serum (FBS) also facilitated sustained release of **gold-1a** from **1-SP-gold-1a** (Supporting Information Figure S18). Complexes **1** and **2** could both interact with FBS (Supporting Information Figure S19), but unlike FBS, other reagents in cell culture medium such as L-glutamine and penicillin–streptomycin could not trigger release.

The in vitro cytotoxicity of **1-SP-gold-1a** and **gold-1a**-free **1-SP** were evaluated in Transwell 24-well plates. Since the cell culture medium was rich in FBS, which led to the release of **gold-1a**, **1-SP-gold-1a** showed a time-dependent cytotoxic profile with higher cytotoxicity than **1-SP** (without **gold-1a**) toward the cancer cells (Figure 5b). As revealed in our previous work,[10] sustained release of **gold-1a** by using encapsulated materials would give improved in vivo anticancer efficacy compared to free **gold-1a**. Thus, **1-SP** could help **gold-1a**, and in principle other cytotoxic agents, by modulating their cytotoxicity in vivo and in reducing side toxicity through localized drug delivery.

In summary, we have reported a self-assembled supramolecular polymer formed by the Au^{III} complex **1** of 2,6-diphenylpyridine and 2,4-diamino-6-(4-pyridyl)-1,3,5-triazine (4-dpt). This Au^{III} supramolecular polymer (**1-SP**) shows distinctive physical features including concentration-dependent specific viscosity and formation of nanofibrillar networks. Polymer **1-SP** displayed sustained cytotoxicity and selective cytotoxicity toward cancerous cells. It can also encapsulate other cytotoxic agents such as $[Au^{III}(TPP)]Cl$ (**gold-1a**) to achieve sustained-release behavior.

Received: December 1, 2011
Revised: February 13, 2012
Published online: April 3, 2012

Keywords: drug delivery · gold · nanostructures · self-assembly · supramolecular polymers

[1] a) D. Astruc, E. Boisselier, C. Ornelas, *Chem. Rev.* **2010**, *110*, 1857; b) D. E. Bergbreiter, J. Tian, C. Hongfa, *Chem. Rev.* **2009**, *109*, 530; c) M. J. Wilkinson, P. W. N. M. van Leeuwen, J. N. H. Reek, *Org. Biomol. Chem.* **2005**, *3*, 2371; d) B. Xing, M.-F. Choi, B. Xu, *Chem. Eur. J.* **2002**, *8*, 5028; e) G. E. Oosterom, J. N. H. Reek, P. C. J. Kamer, P. W. N. M. van Leeuwen, *Angew. Chem.* **2001**, *113*, 1878; *Angew. Chem. Int. Ed.* **2001**, *40*, 1828.

[2] a) M. Shirakawa, N. Fujita, T. Tani, K. Kaneko, M. Ojima, A. Fujii, M. Ozaki, S. Shinkai, *Chem. Eur. J.* **2007**, *13*, 4155; b) A. Kishimura, T. Yamashita, T. Aida, *J. Am. Chem. Soc.* **2005**, *127*, 179; c) J. B. Beck, S. J. Rowan, *J. Am. Chem. Soc.* **2003**, *125*, 13922.

[3] a) A. Dawn, T. Shiraki, S. Haraguchi, S.-i. Tamaru, S. Shinkai, *Chem. Asian J.* **2011**, *6*, 266; b) Y. Chen, K. Li, W. Lu, S. S.-Y. Chui, C.-W. Ma, C.-M. Che, *Angew. Chem.* **2009**, *121*, 10093; *Angew. Chem. Int. Ed.* **2009**, *48*, 9909; c) W. Lu, Y. Chen, V. A. L. Roy, S. S.-Y. Chui, C.-M. Che, *Angew. Chem.* **2009**, *121*, 7757; *Angew. Chem. Int. Ed.* **2009**, *48*, 7621; d) T. Tu, W. Assenmacher, H. Peterlik, R. Weisbarth, M. Nieger, K. H. Dötz, *Angew. Chem.* **2007**, *119*, 6486; *Angew. Chem. Int. Ed.* **2007**, *46*, 6368; e) M. Shirakawa, N. Fujita, T. Tani, K. Kaneko, S. Shinkai, *Chem. Commun.* **2005**, 4149; f) K. Kuroiwa, T. Shibata, A. Takada, N. Nemoto, N. Kimizuka, *J. Am. Chem. Soc.* **2004**, *126*, 2016; g) S.-i. Kawano, N. Fujita, S. Shinkai, *J. Am. Chem. Soc.* **2004**, *126*, 8592; h) V. W.-W. Yam, R. P.-L. Tang, K. M.-C. Wong, K.-K. Cheung, *Organometallics* **2001**, *20*, 4476; i) P. Terech, C. Chachaty, J. Gaillard, A. M. Giroud-Godquin, *J. Phys.* **1987**, *48*, 663.

[4] S. R. Bull, M. O. Guler, R. E. Bras, T. J. Meade, S. I. Stupp, *Nano Lett.* **2005**, *5*, 1.

[5] a) A. Bindoli, M. P. Rigobello, G. Scutari, C. Gabbiani, A. Casini, L. Messori, *Coord. Chem. Rev.* **2009**, *253*, 1692; b) X. Wang, Z. Guo, *Dalton Trans.* **2008**, 1521; c) P. C. A. Bruijnincx, P. J. Sadler, *Curr. Opin. Chem. Biol.* **2008**, *12*, 197; d) D. Saggioro, M. P. Rigobello, L. Paloschi, A. Folda, S. A. Moggach, S. Parsons, L. Ronconi, D. Fregona, A. Bindoli, *Chem. Biol.* **2007**, *14*, 1128; e) C. X. Zhang, S. J. Lippard, *Curr. Opin. Chem. Biol.* **2003**, *7*, 481; f) C. F. Shaw III, *Chem. Rev.* **1999**, *99*, 2589.

[6] a) C.-M. Che, R. W.-Y. Sun, *Chem. Commun.* **2011**, *47*, 9554; b) K. H.-M. Chow, R. W.-Y. Sun, J. B. B. Lam, C. K.-L. Li, A. Xu, D.-L. Ma, R. Abagyan, Y. Wang, C.-M. Che, *Cancer Res.* **2010**, *70*, 329; c) R. W.-Y. Sun, C. K.-L. Li, D.-L. Ma, J. J. Yan, C.-N. Lok, C.-H. Leung, N. Zhu, C.-M. Che, *Chem. Eur. J.* **2010**, *16*, 3097; d) R. W.-Y. Sun, C.-M. Che, *Coord. Chem. Rev.* **2009**, *253*, 1682; e) Y. Wang, Q.-Y. He, R. W.-Y. Sun, C.-M. Che, J.-F. Chiu, *Cancer Res.* **2005**, *65*, 11553; f) C.-M. Che, R. W.-Y. Sun, W.-Y. Yu, C.-B. Ko, N. Zhu, H. Sun, *Chem. Commun.* **2003**, 1718.

[7] E. Rabinovich, I. Goldberg, Z. Gross, *Chem. Eur. J.* **2011**, *17*, 12294.

[8] a) J. J. Yan, A. L.-F. Chow, C.-H. Leung, R. W.-Y. Sun, D.-L. Ma, C.-M. Che, *Chem. Commun.* **2010**, *46*, 3893; b) C. K.-L. Li, R. W.-Y. Sun, S. C.-F. Kui, N. Zhu, C.-M. Che, *Chem. Eur. J.* **2006**, *12*, 5253.

[9] R. W.-Y. Sun, D.-L. Ma, E. L.-M. Wong, C.-M. Che, *Dalton Trans.* **2007**, 4884.

[10] J. J. Yan, R. W.-Y. Sun, P. Wu, M. C. M. Lin, A. S.-C. Chan, C.-M. Che, *Dalton Trans.* **2010**, *39*, 7700.

[11] P. Casuso, P. Carrasco, I. Loinaz, H. J. Grande, I. Odriozola, *Org. Biomol. Chem.* **2010**, *8*, 5455.

[12] a) M. Maeda, M. Ligo, H. Tsuda, H. Fujita, Y. Yonemura, K. Nakagawa, Y. Endo, T. Sasaki, *Anti-Cancer Drug Des.* **2000**, *15*, 217; b) C.-W. Chan, D. M. P. Mingos, A. J. P. White, D. J. Williams, *Polyhedron* **1996**, *15*, 1753.

[13] T. Mosmann, *J. Immunol. Methods* **1983**, *65*, 55.

[14] a) H. Graf, C. Jüngst, G. Straub, S. Dogan, R.-T. Hoffmann, T. Jakobs, M. Reiser, T. Waggershauser, T. Helmberger, A. Walter, A. Walli, D. Seidel, B. Göke, D. Jüngst, *Digestion* **2008**, *78*, 34; b) W. Y. Lau, S. C. H. Yu, E. C. H. Lai, T. W. T. Leung, *J. Am. Coll. Surg.* **2006**, *202*, 155.

